JCTC Journal of Chemical Theory and Computation

Article

pubs.acs.org/JCTC

Double Hybrid Functionals and the Π-System Bond Length Alternation Challenge: Rivaling Accuracy of Post-HF Methods

Michael Wykes,*[,†] Neil Qiang Su,[‡] Xin Xu,[‡] Carlo Adamo,[§,∥] and Juan-Carlos Sancho-García[⊥]

[†]Madrid Institute for Advanced Studies, IMDEA Nanoscience, Calle Faraday 9, Campus Cantoblanco, 28049 Madrid, Spain

[‡]Shanghai Key Laboratory of Molecular Catalysis and Innovative Materials, MOE Laboratory for Computational Physical Science, Department of Chemistry, Fudan University, Shanghai 200433, China

[§]Institut de Recherche de Chimie Paris, IRCP CNRS UMR-8247, École Nationale Superieure de Chimie de Paris, Chimie ParisTech, 11 rue P. et M. Curie, F-75231 Paris Cedex 05, France

[∥]Institut Universitaire de France, 103 Boulevard Saint Michel, F-75005 Paris, France

[⊥]Departamento de Química Física, Universidad de Alicante, E-03080 Alicante, Spain

Supporting Information

ABSTRACT: Predicting accurate bond length alternations (BLAs) in long conjugated oligomers has been a significant challenge for electronic-structure methods for many decades, made particularly important by the close relationships between BLA and the rich optoelectronic properties of π-delocalized systems. Here, we test the accuracy of recently developed, and increasingly popular, double hybrid (DH) functionals, positioned at the top of *Jacobs Ladder* of DFT methods of increasing sophistication, computational cost, and accuracy, due to incorporation of MP2 correlation energy. Our test systems comprise oligomeric series of polyacetylene, polymethineimine, and polysilaacetylene up to six units long. MP2 calculations reveal a pronounced shift in BLAs between the 6-31G(d) basis set used in many studies of BLA to date and the larger cc-pVTZ basis set, but only modest shifts between cc-pVTZ and aug-cc-pVQZ results. We hence perform new reference CCSD(T)/cc-pVTZ calculations for all three series of oligomers against which we assess the performance of several families of DH functionals based on BLYP, PBE, and TPSS, along with lower-rung relatives including global- and range-separated hybrids. Our results show that DH functionals systematically improve the accuracy of BLAs relative to single hybrid functionals. xDH-PBE0 (N^4 scaling using SOS-MP2) emerges as a DH functional rivaling the BLA accuracy of SCS-MP2 (N^5 scaling), which was found to offer the best compromise between computational cost and accuracy the last time the BLA accuracy of DFT- and wave function-based methods was systematically investigated. Interestingly, xDH-PBE0 (XYG3), which differs to other DHs in that its MP2 term uses PBE0 (B3LYP) orbitals that are not self-consistent with the DH functional, is an outlier of trends of decreasing average BLA errors with increasing fractions of MP2 correlation and HF exchange.

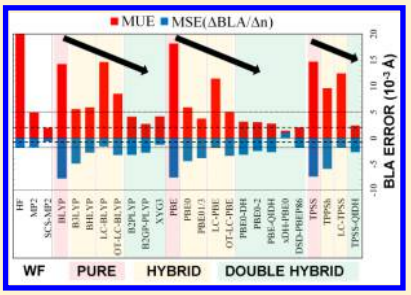

INTRODUCTION

Bond length alternation (BLA) is a geometrical parameter defined as the difference in bong length between a single bond and an adjacent double or triple bond and is closely related to many optoelectronic properties of π-delocalized systems, including electronic (and hence optical) band gaps,[1,2] polarizabilities,[3,4] two-photon absorption efficiencies,[5] and photochromic properties.[6] Simple as it seems, accurately describing BLA is a challenge for many electronic structure methods. Trans-polyacetylene (referred to here as CC-II) is the most intensively studied system. It is well known that Hartree−Fock (HF) overestimates BLA in CC-II, while schemes based on pure density functional theory (DFT), for example, BLYP,[7,8] leads to the opposite error.[9] In terms of post-HF methods, second-order Møller−Plesset (MP2) provides improved accuracy for CC(II) BLA, although this method slightly underestimates the BLA and overestimates the rate of decrease in BLA with increasing chain length[10−12] (Figure 3), while spin-component-scaled MP2 (SCS-MP2)[13] is in better agreement with CCSD(T).[11,14] As underestimation of BLA by pure DFT approaches can be traced to self-interaction errors,[15,16] self-interaction corrected DFT schemes[15] and global hybrid[9,11,14,17,18] and range-separated hybrid functionals[10,14,19,20] show improved performance. Interestingly, upon optimization of the range parameter (considered by some to be an unavoidable step[21] when studying π-conjugated materials), the rate at which BLA decreases with increasing chain length is severely overestimated.[16] Systematic studies over oligomeric series of several other polymers have allowed their division into three phenomenological categories:[14,18,22] In type-I oligomers (e.g., CSi-I, Figure 1), the BLA decreases exponentially with chain length and rapidly converges to zero. Symmetric type-II oligomers (e.g., CC-II) exhibit nonzero BLA for all chain lengths due to Peierls distortion. Finally, asymmetric type-III oligomers (e.g., CN-III) present a large BLA for all chain

Received: November 4, 2014
Published: December 19, 2014

© 2014 American Chemical Society

DOI: 10.1021/ct500986b
J. Chem. Theory Comput. 2015, 11, 832−838

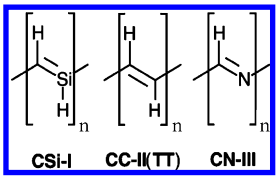

Figure 1. Representation of the oligomers considered in this study. All chains are capped by terminal hydrogen atoms. *n* is the number of repeat units.

lengths. A study published three years ago by one of us (C.A.) presented a thorough assessment of the ability of many DFT and wave function methods to correctly describe BLA across these three categories of systems, using CCSD(T) as a reference.[14] Although trends in BLA errors for each method tested were found to vary significantly between different oligomer series, a few general trends were nevertheless identified: HF was found to overestimate BLA with mean absolute deviations (MAD) of about 3×10^{-2} Å. MP4(SDQ) and CCSD also overestimated BLA, but to a lesser extent (MAD about 1×10^{-2} Å). MP2, MP4, and spin-component-scaled (SCS-)MP2[13] generally produced accurate BLAs (MAD about 5×10^{-3} Å), the two former (the latter) slightly underestimating (overestimating) the reference data. None of the tested DFT functionals were able to compete with MP2, MP4, and SCS-MP2 across the full set of molecules. Indeed, for long oligomers, global hybrids including a large share to exact exchange (BH&HLYP[23] or M06-2X[24]) or a range-separated hybrid (CAM-B3LYP[25]) were found to provide the best results, while for the shortest oligomers, B3LYP[26] and B2PLYP[27] performed well. The latter is the first example of a modern double hybrid (DH) functional which, in addition to a fraction of exact HF exchange, includes MP2 correlation energy. Improvements in accuracy afforded by early double hybrids such as B2PLYP have fueled the development of many more (see refs 28 and 29 for recent reviews). In this study, we subject some of the most accurate and recently developed DHs to the BLA test using the most representative example of each class of oligomers shown in Figure 1.

DOUBLE HYBRID FUNCTIONALS

Following the pioneering studies of Ernzerhof[30] and Truhlar,[31] the first modern double hybrid functional, B2-PLYP, was developed by Grimme in 2006.[27] B2-PLYP and related functionals can be expressed using a simple formula, similar to that used for global hybrids such as B3LYP[26]

$$E_{XC}^{DH} = (1 - a_X)E_X^{DFT} + a_X E_X^{HF} + (1 - a_C)E_C^{DFT} + a_C E_C^{MP2} \quad (1)$$

where E_X^{DFT} and E_C^{DFT} are, respectively, the DFT-exchange and correlation energies, and E_X^{HF} and E_C^{MP2} are the HF exchange and MP2 perturbative correlation energy, both computed on the basis of DFT orbitals. E_X^{HF} and E_C^{MP2} are scaled by the parameters a_X and a_C. In B2-PYLP, a_X and a_C take values of 0.53 and 0.27, respectively, obtained by fitting to small-molecule heats of formation. Since the development of B2-PLYP, many more DHs have been developed.[28,29] Apart from the use of different DFT exchange and correlation functionals, DHs can be chiefly distinguished by the strategy employed to determine the mixing parameters a_X and a_C and the type of MP2 term used. The former allows DHs to be divided into empirical functionals, whose parameters are determined by fitting to reproduce benchmark data, and non-empirical (or *parameter-free*) functionals, whose parameters are determined according to theoretical considerations. The MP2 term allows distinction between DHs employing a conventional MP2-type term in which correlation energy contributions of electron pairs with the same and opposite spin are given the same weights and spin-component-scaled (SCS) approaches in which they are given different weights.[13] The spin-opposite-scaled (SOS) MP2 term is a special case of SCS in which the same spin component is ignored (thus bringing down the formal scaling from N^5 to N^4, where N is the number of basis functions).[32] Another distinction is what orbitals are used in the MP2 calculation. While most DHs, like B2PLYP, use orbitals obtained from a self-consistent calculation using the conventional hybrid functional defined by the first three terms in eq 1 (i.e., DH functional itself, but without the MP2-term), DHs have been developed that use B3LYP[33] or PBE0[34] orbitals for the MP2 calculation. In this study, we have selected a range of functionals summarized in Table 1.

Methods. Geometry optimizations were performed using the DHs shown in Table 1, as well as the pure functionals BLYP,[7,8] PBE,[40] and TPSS;[41] global hybrid functionals B3LYP,[26] BH&HLYP,[23] PBE0,[42,43] PBE01/3,[44] and TPSSh;[41] and range-separated hybrids[45] LC-BLYP, LC-PBE, and LC-TPSS. The latter three LC functionals were tested using both

Table 1. Functionals Used in This Study, as Defined in Eq 1

name	year	DFT_X	DFT_C	a_X	a_C	a_{Co} [†]	a_{Cs} [‡]
Empirical							
B2-PLYP[27]	2006	B88	LYP	0.53	0.27		
B2GP-PLYP[35]	2008	B88	LYP	0.65	0.36		
XYG3[33§]	2009	B88	LYP	0.8	0.32		
DSD-PBEP86[36‖]	2011	PBE	P86	0.7	0.43	0.53	0.25
xDH-PBE0[34⊥]	2012	PBE	PBE	0.83	0.54	0.54	0
Nonempirical							
PBE0-DH[37]	2011	PBE	PBE	0.5	0.125		
PBE0−2[38]	2012	PBE	PBE	0.79	0.5		
PBE-QIDH[39]	2014	PBE	PBE	0.693	0.333		
TPSS-QIDH[39]	2014	TPSS	TPSS	0.693	0.333		

[†] a_{Co} is the opposite spin scaling factor for SCS and SOS MP2 terms. (a_C does not affect the MP2 terms, but $(1 - a_C)$ still scales the DFT correlation). [‡] a_{Cs} is the same spin scaling factor for SCS MP2 terms. [§]Uses B3LYP orbitals in MP2 term. [‖]Uses SCS-MP2 term and D3 dispersion corrections. [⊥]Uses SOS-MP2 term with PBE0 orbitals.

DOI: 10.1021/ct500986b
J. Chem. Theory Comput. 2015, 11, 832−838

fixed values of the range separation parameter μ and values tuned for each oligomer so as to minimize the difference between the highest occupied molecular orbital energy and the ΔSCF ionization potential (IP), defining OT-LC functionals.[46] OT-LC-optimized geometries were obtained by iterating between cycles of IP tuning and geometry optimization to self-consistency. LC functionals employing a fixed μ used the value of 0.47 $Bohr^{-1}$ proposed by Hirao et al.[45] rather than the conventional choice of 0.33 used in one of our previous studies on BLA.[14] The value of 0.47 $Bohr^{-1}$ was chosen as a recent study of polarizabilities, and the second hyperpolarizabilities (which are closely linked to BLA) in conjugated oligomeric series demonstrated that a μ of 0.47 $Bohr^{-1}$ provided better results than 0.33 $Bohr^{-1}$.[47] All calculations were performed with the Gaussian09[48] program, with the exception of and XYG3 and xDH-PBE0 calculations, which were performed using a development version of NWChem[49] and MP2, SCS-MP2, and CCSD(T) calculations, which were performed using the RICC2 module of Turbomole.[50] The latter employs the resolution of identity (RI) approximation in the post-HF correlation calculations. Test calculations on all the oligomers considered in this work demonstrated that full MP2 (performed with Gaussian 09) and RI-MP2 BLAs differ by less than 10^{-4} Å, justifying the use of the RI approximation in all our other MP2, SCS-MP2, and CCSD(T) calculations. All post-HF and DH calculations relied on the frozen core approximation. We systematically employed a tightened SCF threshold (10^{-9} for MP2, SCS-MP2, and CCSD(T), 10^{-8} au elsewhere) and geometry optimization criteria (RMS force smaller than 10^{-5} au). All calculations relied on analytical gradients, with the exception of CCSD(T), which used numerical gradients. Geometry optimizations took advantage of the maximal molecular symmetry present (C_{2h} for CC, C_s for CN and CSi). Note that all the chains of Figure 1 are capped by terminal hydrogen atoms in our calculations, and BLAs were measured at the center of the oligomers. The cc-pVTZ basis set was employed for all calculations, following MP2 test calculations with larger basis sets (see below). All optimized geometries generated in this study are available in .xyz format as part of the Supporting Information. The SIE11 data presented in Figure 7 are those reported in previous studies,[39,51] with the exception of those for xDH-PBE0 which were computed using the GTlarge basis set.

Basis Set Effects. As the choice of basis set can significantly impact results, we performed tests on the 6-31G(d) basis set used in several studies on BLA to date[14,18,22] as well as the larger (aug-)cc-pVTZ and (aug-)cc-pVQZ basis sets. Tests were performed with MP2 calculations, as these were found to be more sensitive to basis set than DH DFT methods, and should provide an indicator for the basis-set dependence of the more computationally demanding CCSD(T) calculations. The results are shown in Figure 2, highlighting a significant shift between 6-31G(d) and cc-pVTZ results for all three systems, which is particularly severe for CSi. The impact of the resolution of identity (RI) approximation on BLAs obtained from RI-MP2[52] was assessed, and the MP2/cc-pVTZ and RI-MP2/cc-pVTZ curves were found to be indistinguishable. Hence, the RI approximation was used in all subsequent CCSD(T) and MP2 calculations (but not in the MP2 part of DH calculations). For CC and CN, cc-pVTZ and cc-pVQZ curves are superimposed and do not deviate significantly from aug-cc-pVTZ and aug-cc-pVQZ curves, while for CSi, cc-pVTZ does not deviate significantly from the aug-cc-pVTZ, cc-pVQZ,

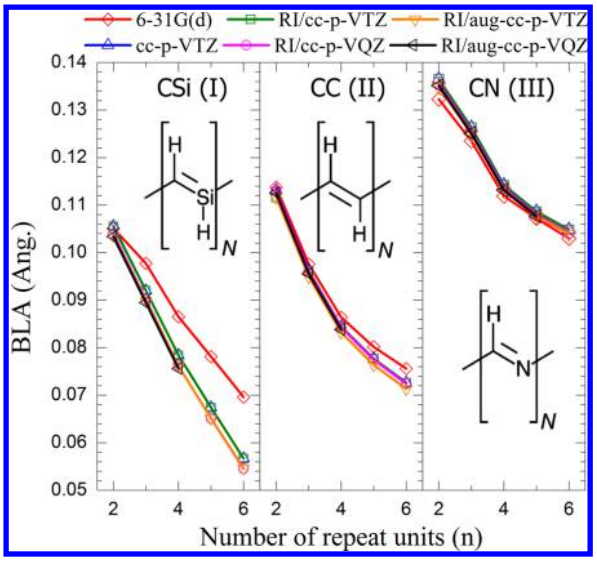

Figure 2. Basis set dependence of MP2 BLAs, showing that while 6-31G(d) BLAs are far from converged with respect to basis set (especially for CSi), cc-pVTZ BLAs are sufficiently close to being converged to allow for accurate conclusions to be made.

and aug-cc-pVQZ curves, which are superimposed. This suggests that BLAs obtained with cc-pVTZ are almost converged with respect to basis set and will thus represent a good balance between accuracy and computational cost. As far as we aware, this is the first time that reference CCSD(T) calculations for a series of oligomers of increasing length have utilized the cc-pVTZ basis set for these systems.

Wave Function Results. Figure 3 shows HF, MP2, SCS-MP2 (n=2 to n-6) and CCSD(T) (n=2 to n=4) BLAs obtained

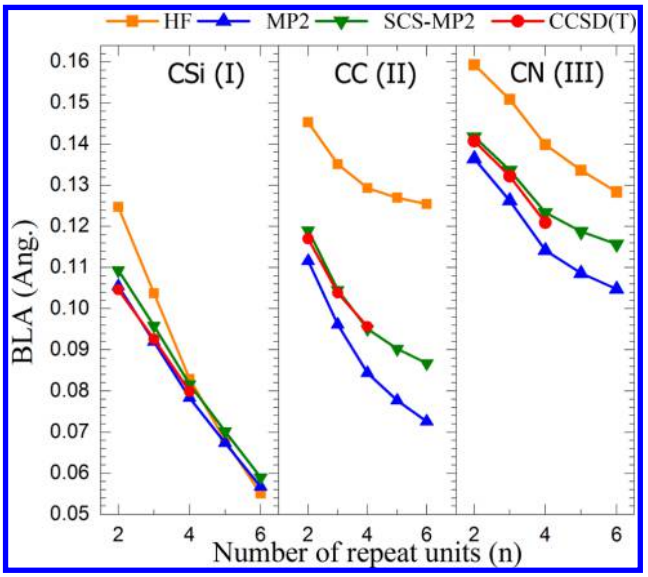

Figure 3. HF, MP2, SCS-MP2, and CCSD(T) BLAs, all using the cc-pVTZ basis set.

with the cc-pVTZ basis set. HF is found to strongly overestimate BLA for CC(II) and CN(III) for all n considered and for short oligomers of CSi(I) (for which the HF BLA decreases far too rapidly). MP2 underestimates BLA in CC(II) and CN(III) (and the BLA decreases too rapidly with chain length), while SCS-MP2 is in good agreement with the

DOI: 10.1021/ct500986b
J. Chem. Theory Comput. 2015, 11, 832−838

available CCSD(T) results. MP2 and SCS-MP2 results are similarly faithful to the CCSD(T) results for CSi, though MP2 is slightly more accurate.

Double Hybrid Results. In order to assess the performance of each method, here, we focus on the errors relative to CCSD(T) BLAs for the oligomers n = 2 to n = 4. Plots and tables of the full set of BLA results can be found in the Supporting Information. A first glance at Figure 4 (and Figures

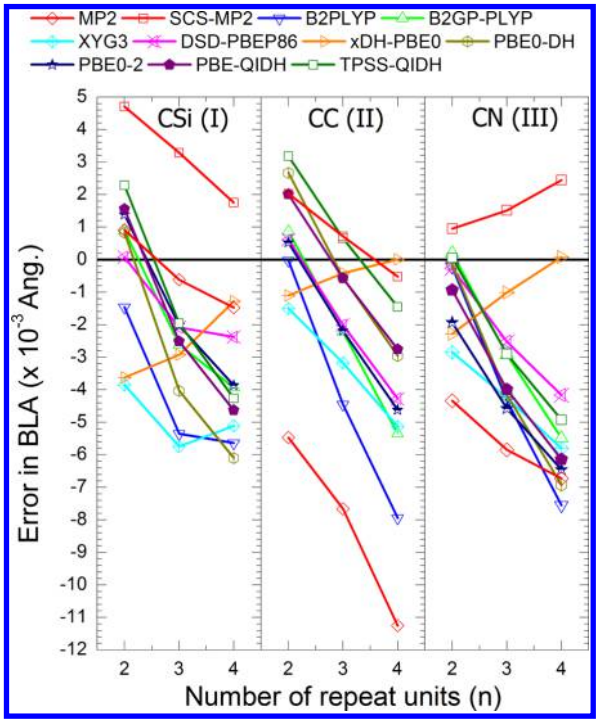

Figure 4. Errors in DH BLAs relative to CCSD(T) results.

S1 and S2, Supporting Information) suggests that all of the DHs tested provide quite accurate BLAs, with DH curves mainly falling in between SCS-MP2 and MP2 results for CC and CN, and competitive with SCS-MP2 for CSi with absolute errors lower than 6×10^{-3} Å. However, as a general trend, it appears that the BLA decreases too rapidly with chain length, meaning that errors in BLA grow rapidly with chain length. To quantify such errors, we define a metric for the change in BLA with chain length, $\Delta\mathrm{BLA}/\Delta n = 1/2(\mathrm{BLA}(n = 4) - \mathrm{BLA}(n = 2))$, as well as defining its associated error: $E(\Delta\mathrm{BLA}/\Delta n) = \Delta\mathrm{BLA}/\Delta n - \Delta\mathrm{BLA}^{\mathrm{CCSD(T)}}/\Delta n$. Mean signed $E(\Delta\mathrm{BLA}/\Delta n)$ (MSE(ΔBLA/Δn)) values and mean unsigned errors (MUEs) relative to CCSD(T) results are summarized in in Figures 5 and 6 and are tabulated in the Supporting Information. All the DHs as well as (SCS-)MP2 suffer from a too rapid decrease in BLA with chain length ($E(\Delta\mathrm{BLA}/\Delta n) < 0$), with the exception of xDH-PBE0, for which the decrease in BLA is too slow ($E(\Delta\mathrm{BLA}/\Delta n) > 0$). Interestingly, xDH-PBE0 is also the most accurate DH with mean (unsigned) deviations relative to CCSD(T) of −14 (14) pm, which outperforms even SCS-MP2 with values of 19 (20) pm. Comparing DH performance across the different series (Figure 5), it is shown that xDH-PBE0 provides both the smallest MUEs and MSE(ΔBLA/Δn) values for both CC and CN. For CSi, however, a related functional XYG3 yields the smallest MSE(ΔBLA/Δn) of −6 pm per unit (though with relatively large MUE of 49 pm, while DSD-PBEP86 seems to provide the most balanced description with

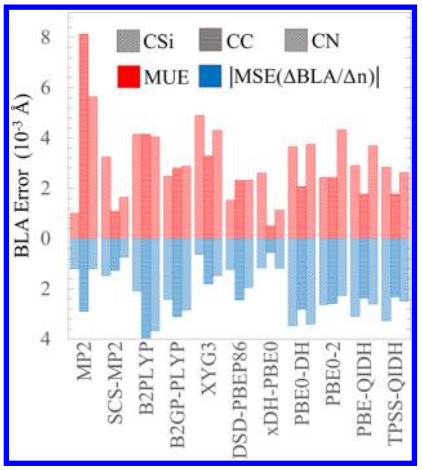

Figure 5. Average BLA MUE and MSE(ΔBLA/Δn) for each oligomer series. For clarity, the absolute value of MSE(ΔBLA/Δn) has been plotted (affecting the sign of xDH-PBE0 for all three series and SCS-MP2 for CN).

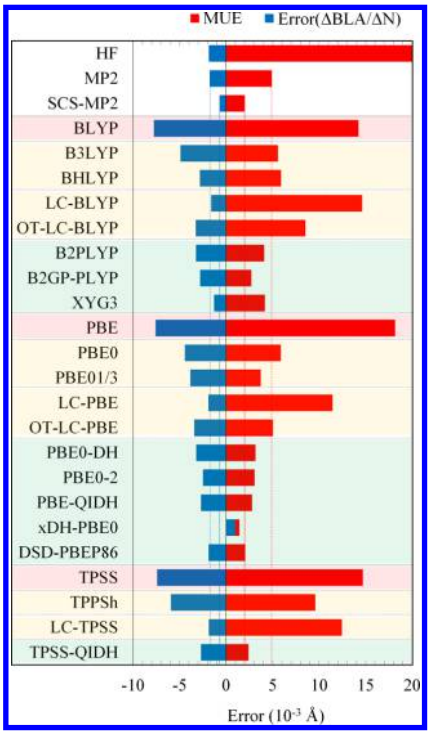

Figure 6. Average BLA MUE and MSE(ΔBLA/Δn) across all the methods tested. Pure DFT functionals are highlighted in red, (single) hybrid functionals in yellow, and DH functionals in green. Vertical colored lines facilitate comparison of each method with (SCS) MP2.

the smallest MUE (15 pm) and a modest MSE(ΔBLA/Δn) of −12 pm per unit. However, xDH-PBE0 comes close to this, with the same MSE(ΔBLA/Δn) of −12 pm and a only a slightly higher MUE of 26 pm. This excellent performance of xDH-PBE0 in describing BLA is consistent with previous findings that xDH-PBE0 provides accurate geometries, generally more accurate than PBE0-DH and PBE0-2.[53]

In an attempt to rationalize DH performance, we looked for trends in MUEs, mean signed errors (MSEs) and MSE(ΔBLA/Δn) errors as a function of the weight of HF exchange (a_X) and MP2 correlation energy (a_C) in each DH. The only clear-cut trend to emerge is of an improved ΔBLA/Δn for higher

DOI: 10.1021/ct500986b
J. Chem. Theory Comput. 2015, 11, 832−838

fractions of MP2 correlation and HF exchange (Figure 7), which is consistent with previous findings that a high (average)

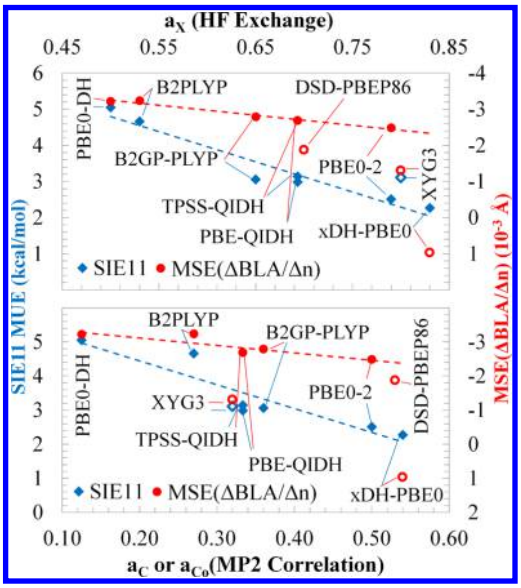

Figure 7. MSE(ΔBLA/Δn) and SIE11 errors vs the fraction of HF exchange and MP2 correlation (in the case of SCS- or SOS-MP2, the fraction of opposite spin correlation) present in each DH. Dashed lines are linear fits to filled points; unfilled points are not included in the linear fit.

fraction of HF is important for describing BLA in longer oligomers with global (range-separated) hybrids.[11,14] High fractions of HF exchange are important for reducing self-interaction errors, which have a direct impact on delocalization and BLA.[15,16] MUEs across the SIE11[51] benchmark are specifically designed to test self-interaction errors; those DHs for which results are available[39] are also plotted in Figure 7, confirming that the SIE errors are indeed decreased with increasing MP2 correlation and HF exchange. Interestingly, however, XYG3 and xDH-PBE0, the two functionals using nonself-consistent B3LYP and PBE0 orbitals, respectively, in their MP2 terms are outliers of the trends, providing much smaller MSE(ΔBLA/Δn) than the trend would predict (however at the price of larger SIE MUE). It is also interesting to note that empirical and nonempirical groups (as defined in Table 1) perform similarly well, with neither group having a clear advantage. Finally, we compare the performance of DHs against lower-rung pure global hybrid and range-separated hybrids to assess whether DHs represent a significant improvement over these functionals of lower computational cost. We tested range-separated hybrids using both fixed values of the range separation parameter (μ = 0.47 Bohr^{-1}) and optimally tuned (OT) μ values chosen separately for each oligomer to minimize the difference between the highest occupied molecular orbital energy and the ionization potential (see Methods section for details). Figure 6 presents a summary of the performance across pure, hybrid, and DH functionals. Results are grouped into families employing the same DFT exchange and correlation functionals. These results show that DHs are indeed more accurate than their lower-rung counterparts, with consistently the lowest MUEs and some of the lowest MSE(ΔBLA/Δn) values. However, some of the hybrid functionals with high fractions of HF exchange, namely, BH&HLYP and the nontuned LC functionals, feature lower MSE(ΔBLA/Δn) values than some of their DH counterparts. Nevertheless, the DHs XYG3 and xDH-PBE0 still feature the smallest MSE(ΔBLA/Δn) within the BLYP and PBE families, respectively. It is interesting to note the effect of tuning on the performance of LC functionals. Nontuned LC functionals significantly overestimate BLA (resulting in large MUEs) but feature an error that is relatively constant with chain length (resulting in low MSE(ΔBLA/Δn) values). Upon tuning, μ, and hence the fraction of HF exchange at short range, decreases with increasing chain length. For n = 2, OT-LC-BLYP μ values for CSi, CC, and CN are 0.27, 0.33, and 0.36 Bohr^{-1}, respectively, while at n = 6, they are 0.21, 0.22, and 0.26 Bohr^{-1}. Tuned μ values for all oligomer lengths for both OT-LC-BLYP and OT-LC-PBE can be found in the Supporting Information.

This reduces MUEs, but it comes at the expense of increased MSE(ΔBLA/Δn).[16] Recent studies have shown that LC-tuned functionals provide no improvement in calculated optical bandgaps[54] and polarizabilities and second hyperpolarizabilities[47] of series of conjugated oligomers, as they overestimate changes with chain length to a greater extent than nontuned functionals. So while the tested LC hybrids can provide either small MUEs (tuned) or accurate ΔBLA/Δn (nontuned), our results show that the tested DHs provide both.

Conclusions. In this study, we assess the performance of several recently developed double hybrid functionals when applied to the challenging problem of describing bond length alternation in conjugated oligomers (in our case, oligomeric series of polyacetylene, polymethineimine, and polysilaacetylene up to six units long). We perform a careful analysis of basis set effects and find a pronounced shift in BLAs between the 6-31G(d) basis set used in many studies of BLA to date and the larger cc-pVTZ basis set, although with only modest shifts between cc-pVTZ and aug-cc-pVQZ results. Our CCSD(T)/cc-pVTZ calculations for all three series of oligomers are used as new reference data against which we assess the performance of several families of DH functionals based on BLYP, PBE, and TPSS, along with lower-rung relatives including global- and range-separated hybrids (the latter employing both constant and optimally tuned range separation parameters). Our results show that DH functionals systematically improve the accuracy of BLAs relative to single hybrid functionals, consistently providing smaller MUEs than single hybrid functionals and MP2, and ΔBLA/Δn (slopes in BLA vs chain length) competitive with the best single hybrid functionals. It is furthermore worth highlighting that while the tested LC hybrids can provide either small MUEs (employing tuned range separation parameters) or accurate ΔBLA/Δn (employing nontuned μ = 0.47), our results show that the tested DHs provide both small MUEs and accurate ΔBLA/Δn. xDH-PBE0 (N^4 scaling using SOS-MP2) emerges as a DH functional rivaling the BLA accuracy of SCS-MP2 (N^5 scaling), which was found to offer the best compromise between computational cost and accuracy the last time the BLA accuracy of DFT- and wave function-based methods was systematically investigated.[14]

Our finding that xDH-PBE0 produces particularly accurate BLAs is consistent with previous studies indicating that xDH-PBE0 generally provides accurate geometries (which are slightly more accurate than PBE0-DH and PBE0−2 geometries).[53] DHs with the highest fractions of MP2 correlation and HF exchange were found to provide the most accurate ΔBLA/Δn, consistent with similar findings for the fraction of HF exchange in global and range-separated hybrids.[14] Interestingly, xDH-PBE0 (XYG3), which differs to other DHs in that its MP2 term

DOI: 10.1021/ct500986b
J. Chem. Theory Comput. 2015, 11, 832−838

uses PBE0 (B3LYP) orbitals that are not self-consistent with the DH functional, is an outlier of trends of decreasing average $\Delta BLA/\Delta n$ errors with increasing (decreasing) MP2 correlation and HF exchange (self-interaction errors). Surprisingly, these two functionals suffer from larger self-interaction errors (over the SIE11 test-set), but smaller errors in $\Delta BLA/\Delta n$ than would be expected based on their fraction of MP2 correlation and HF exchange. This is consistent with previous findings that reducing self-interaction errors does not necessarily reduce $\Delta BLA/\Delta n$ errors.[16]

■ ASSOCIATED CONTENT

Supporting Information

Plots of BLA vs n for all DHs, tabulated BLA, and error data for all methods. SIE11 errors for xDH-PBE0. Optimized geometries in .xyz format. This material is available free of charge via the Internet at http://pubs.acs.org.

■ AUTHOR INFORMATION

Corresponding Author

*E-mail: michael.wykes@imdea.org.

Notes

The authors declare no competing financial interest.

■ ACKNOWLEDGMENTS

The authors thank Éric Brémond (IIT, Genoa, Italy) for the SIE11 data in Figure 7. The work at IMDEA was supported by the Campus of International Excellence (CEI) UAM+CSIC. M.W. thanks the European Commission for his Marie Curie Fellowship (FP7-PEOPLE-2012-IEF-331795). J.-C.S.-G. thanks the Ministerio de Economia y Competitividad of Spain and the European Regional Development Fund through project CTQ2011-27253.

■ REFERENCES

(1) Bredas, J. L. *J. Chem. Phys.* **1985**, *82*, 3808.
(2) Kertész, M. *Chem. Phys.* **1979**, *44*, 349−356.
(3) Murugan, N. A.; Kongsted, J.; Rinkevicius, Z.; Agren, H. *Proc. Natl. Acad. Sci. U.S.A.* **2010**, *107*, 16453−8.
(4) Olsen, S.; McKenzie, R. H. *J. Chem. Phys.* **2011**, *134*, 114520.
(5) Bartkowiak, W.; Zaleśny, R.; Leszczynski, J. *Chem. Phys.* **2003**, *287*, 103−112.
(6) Patel, P. D.; Masunov, A. E. *J. Phys. Chem. A* **2009**, *113*, 8409−14.
(7) Becke, A. D. *Phys. Rev. A* **1988**, *38*, 3098−3100.
(8) Lee, C.; Yang, W.; Parr, R. G. *Phys. Rev. B* **1988**, *37*, 785−789.
(9) Ho Choi, C.; Kertesz, M.; Karpfen, A. *J. Chem. Phys.* **1997**, *107*, 6712.
(10) Jacquemin, D.; Perpète, E. A.; Scalmani, G.; Frisch, M. J.; Kobayashi, R.; Adamo, C. *J. Chem. Phys.* **2007**, *126*, 144105.
(11) Sancho-García, J. C.; Pérez-Jiménez, A. J. *Phys. Chem. Chem. Phys.* **2007**, *9*, 5874−9.
(12) Zhao, Y.; Truhlar, D. G. *J. Phys. Chem. A* **2006**, *110*, 10478−86.
(13) Grimme, S. *J. Chem. Phys.* **2003**, *118*, 9095.
(14) Jacquemin, D.; Adamo, C. *J. Chem. Theory Comput.* **2011**, *7*, 369−376.
(15) Ciofini, I.; Adamo, C.; Chermette, H. *J. Chem. Phys.* **2005**, *123*, 121102.
(16) Körzdörfer, T.; Parrish, R. M.; Sears, J. S.; Sherrill, C. D.; Brédas, J.-L. *J. Chem. Phys.* **2012**, *137*, 124305.
(17) Jacquemin, D.; Femenias, A.; Chermette, H.; Ciofini, I.; Adamo, C.; André, J.-M.; Perpète, E. A. *J. Phys. Chem. A* **2006**, *110*, 5952−9.
(18) Jacquemin, D.; Perpète, E. A.; Ciofini, I.; Adamo, C. *Chem. Phys. Lett.* **2005**, *405*, 376−381.
(19) Chabbal, S.; Jacquemin, D.; Adamo, C.; Stoll, H.; Leininger, T. *J. Chem. Phys.* **2010**, *133*, 151104.
(20) Peach, M. J. G.; Tellgren, E. I.; Salek, P.; Helgaker, T.; Tozer, D. J. *J. Phys. Chem. A* **2007**, *111*, 11930−5.
(21) Körzdörfer, T.; Sears, J. S.; Sutton, C.; Brédas, J.-L. *J. Chem. Phys.* **2011**, *135*, 204107.
(22) Jacquemin, D.; Femenias, A.; Chermette, H.; André, J.-M.; Perpète, E. A. *J. Phys. Chem. A* **2005**, *109*, 5734−41.
(23) Becke, A. D. *J. Chem. Phys.* **1993**, *98*, 1372.
(24) Zhao, Y.; Truhlar, D. G. *Theor. Chem. Acc.* **2007**, *120*, 215−241.
(25) Yanai, T.; Tew, D. P.; Handy, N. C. *Chem. Phys. Lett.* **2004**, *393*, 51−57.
(26) Becke, A. D. *J. Chem. Phys.* **1993**, *98*, 5648.
(27) Grimme, S. *J. Chem. Phys.* **2006**, *124*, 034108.
(28) Goerigk, L.; Grimme, S. *Wiley Interdiscip. Rev. Comput. Mol. Sci.* **2014**, *4*, 576−600.
(29) Sancho-García, J. C.; Adamo, C. *Phys. Chem. Chem. Phys.* **2013**, *15*, 14581−94.
(30) Ernzerhof, M. *Chem. Phys. Lett.* **1996**, *263*, 499−506.
(31) Zhao, Y.; Lynch, B. J.; Truhlar, D. G. *J. Phys. Chem. A* **2004**, *108*, 4786−4791.
(32) Jung, Y.; Lochan, R. C.; Dutoi, A. D.; Head-Gordon, M. *J. Chem. Phys.* **2004**, *121*, 9793−802.
(33) Zhang, Y.; Xu, X.; Goddard, W. A. *Proc. Natl. Acad. Sci. U.S.A.* **2009**, *106*, 4963−8.
(34) Zhang, I. Y.; Su, N. Q.; Brémond, E.; Adamo, C.; Xu, X. *J. Chem. Phys.* **2012**, *136*, 174103.
(35) Karton, A.; Tarnopolsky, A.; Lamère, J.-F.; Schatz, G. C.; Martin, J. M. L. *J. Phys. Chem. A* **2008**, *112*, 12868−86.
(36) Kozuch, S.; Martin, J. M. L. *Phys. Chem. Chem. Phys.* **2011**, *13*, 20104−7.
(37) Brémond, E.; Adamo, C. *J. Chem. Phys.* **2011**, *135*, 024106.
(38) Chai, J.-D.; Mao, S.-P. *Chem. Phys. Lett.* **2012**, *538*, 121−125.
(39) Brémond, E.; Sancho-García, J. C.; Pérez-Jiménez, A. J.; Adamo, C. *J. Chem. Phys.* **2014**, *141*, 031101.
(40) Perdew, J. P.; Burke, K.; Ernzerhof, M. *Phys. Rev. Lett.* **1996**, *77*, 3865−3868.
(41) Tao, J.; Perdew, J.; Staroverov, V.; Scuseria, G. *Phys. Rev. Lett.* **2003**, *91*, 146401.
(42) Adamo, C.; Barone, V. *J. Chem. Phys.* **1999**, *110*, 6158.
(43) Ernzerhof, M.; Scuseria, G. E. *J. Chem. Phys.* **1999**, *110*, 5029.
(44) Guido, C. A.; Brémond, E.; Adamo, C.; Cortona, P. *J. Chem. Phys.* **2013**, *138*, 021104.
(45) Song, J.-W.; Hirosawa, T.; Tsuneda, T.; Hirao, K. *J. Chem. Phys.* **2007**, *126*, 154105.
(46) Baer, R.; Livshits, E.; Salzner, U. *Annu. Rev. Phys. Chem.* **2010**, *61*, 85−109.
(47) Nénon, S.; Champagne, B.; Spassova, M. I. *Phys. Chem. Chem. Phys.* **2014**, *16*, 7083−8.
(48) Frisch, M. J.; Trucks, G. W.; Schlegel, H. B.; Scuseria, G. E.; Robb, M. A.; Cheeseman, J. R.; Scalmani, G.; Barone, V.; Mennucci, B.; Petersson, G. A.; Nakatsuji, H.; Caricato, M.; Li, X.; Hratchian, H. P.; Izmaylov, A. F.; Bloino, J.; Zheng, G.; Sonnenberg, J. L.; Hada, M.; Ehara, M.; Toyota, K.; Fukuda, R.; Hasegawa, J.; Ishida, M.; Nakajima, T.; Honda, Y.; Kitao, O.; Nakai, H.; Vreven, T.; Montgomery, J. A., Jr.; Peralta, P. E.; Ogliaro, F.; Bearpark, M.; Heyd, J. J.; Brothers, E.; Kudin, K. N.; Staroverov, V. N.; Kobayashi, R.; Normand, J.; Raghavachari, K.; Rendell, A.; Burant, J. C.; Iyengar, S. S.; Tomasi, J.; Cossi, M.; Rega, N.; Millam, N. J.; Klene, M.; Knox, J. E.; Cross, J. B.; Bakken, V.; Adamo, C.; Jaramillo, J.; Gomperts, R.; Stratmann, R. E.; Yazyev, O.; Austin, A. J.; Cammi, R.; Pomelli, C.; Ochterski, J. W.; Martin, R. L.; Morokuma, K.; Zakrzewski, V. G.; Voth, G. A.; Salvador, P.; Dannenberg, J. J.; Dapprich, S.; Daniels, A. D.; Farkas, Ö.; Ortiz, J. V.; Cioslowski, J.; Fox, D. J. *Gaussian 09*, revision D.01 ; Gaussian, Inc.: Wallingford, CT, 2009.
(49) Valiev, M.; Bylaska, E.; Govind, N.; Kowalski, K.; Straatsma, T.; Van Dam, H.; Wang, D.; Nieplocha, J.; Apra, E.; Windus, T.; de Jong, W. *Comput. Phys. Commun.* **2010**, *181*, 1477−1489.
(50) TURBOMOLE V6.5 2013, a development of University of Karlsruhe and Forschungszentrum Karlsruhe GmbH, 1989−2007,

DOI: 10.1021/ct500986b
J. Chem. Theory Comput. 2015, 11, 832−838

TURBOMOLE GmbH, since 2007; available from http://www.turbomole.com.
(51) Goerigk, L.; Grimme, S. *J. Chem. Theory Comput.* **2010**, *6*, 107−126.
(52) Weigend, F.; Häser, M. *Theor. Chem. Acc.* **1997**, *97*, 331−340.
(53) Su, N. Q.; Adamo, C.; Xu, X. *J. Chem. Phys.* **2013**, *139*, 174106.
(54) Wykes, M.; Milián-Medina, B.; Gierschner, J. *Front. Chem.* **2013**, *1*, 35.

DOI: 10.1021/ct500986b
J. Chem. Theory Comput. 2015, 11, 832−838